INORGANIC CHEMISTRY
FRONTIERS

REVIEW

View Article Online
View Journal | View Issue

Cite this: *Inorg. Chem. Front.*, 2020, **7**, 2867

Chemical vapor transport growth of bulk black phosphorus single crystals

Muhammad Khurram, Zhaojian Sun, Ziming Zhang and Qingfeng Yan *

Received 16th May 2020,
Accepted 25th June 2020

DOI: 10.1039/d0qi00582g

rsc.li/frontiers-inorganic

Phosphorene, which is designated as a monolayer or a few-layer of orthorhombic black phosphorus (BP), has emerged as a new promising member of the two-dimensional material family. A plethora of exciting applications of phosphorene have been reported based on its intriguing properties. Unfortunately, due to the lack of reliable methods for the direct synthesis of highly crystalline phosphorene, bulk BP single crystals have been the sole precursor to achieve high-quality phosphorene. A chemical vapor transport (CVT) reaction method has been deemed the most successful method for the growth of bulk BP single crystals. Herein, recent progress in the controlled growth of bulk BP single crystals by the CVT reaction is briefly reviewed. The emphasis is focused on the reaction system, nucleation and growth mechanism of the CVT synthesis of bulk BP crystals as well as the recent development in the growth of doped and substituted BP single crystals by the CVT reaction method. The challenges and perspectives ahead of the CVT growth of BP crystals are also pointed out.

1. Introduction

As the 13th discovered element in the present periodic table, phosphorus is extraordinary because of its remarkable variety of allotropes. Among all the known phosphorus allotropes, black phosphorus (BP) is the most stable one under ambient conditions. The bulk form of BP was first reported as early as in 1914 by Bridgman.[1] Although the chemistry of phosphorus has been an intriguing and vivid topic in chemistry and applied science, little research has been done on BP during the past century. Monolayer and few-layer BP (phosphorene) have attracted increasing research interest only recently due to their interesting optical, electronic and catalytic properties.[2–5] Phosphorene has a corrugated and layered structure which is the building block for bulk BP. On the basis of the layer numbers, phosphorene can be classified as monolayer, bilayer, and few-layer phosphorene. Morphologically, phosphorene can be categorized as quantum dots, nanoribbons, nanorods, nanoparticles, nanowires, nanotubes, nanoflakes and microscale flakes. Unlike graphene, in-plane bonding in phosphorene forms a puckered honeycomb layered structure due to sp^3

Department of Chemistry, Tsinghua University, Beijing 100084, China.
E-mail: yanqf@mail.tsinghua.edu.cn

Muhammad Khurram

Muhammad khurram received his master's degree in physical chemistry from Quaid-e-Azam University, Islamabad, Pakistan, in 2014. He is currently a PhD candidate under the supervision of Dr Qingfeng Yan at the Department of Chemistry, Tsinghua University. His research interest focuses on the synthesis and applications of black phosphorus.

Zhaojian Sun

Zhaojian Sun received his B.S. degree from the Wuhan University of Technology, China, in 2017. He is currently a PhD candidate under the supervision of Dr Qingfeng Yan at the Department of Chemistry, Tsinghua University. His research interests are the synthesis and photocatalytic application of modified black phosphorus.

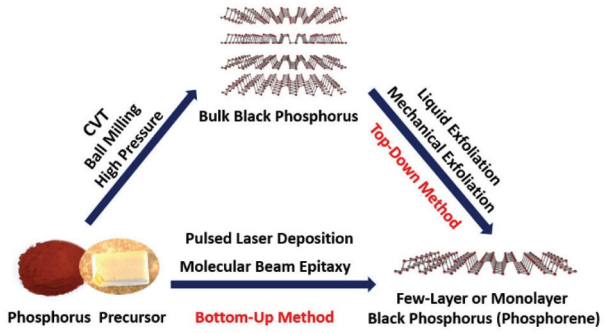

Fig. 1 Schematic illustration of the synthesis of phosphorene.

hybridization of covalently bonded atoms. Phosphorene has a relatively large interlayer spacing as compared to graphene due to its puckered layered structure. Weak interlayer interactions are responsible for holding the phosphorene layers together, which can be easily broken. Phosphorene has a high carrier mobility and a tunable direct band gap. The reliable production of phosphorene with high-quality, large-area and uniform thickness is very important for exploring its properties and potential applications. To enable its successful diverse applications, an easy access to phosphorene is crucial. Motivated by its interesting properties and promising applications, intensive research efforts have been devoted to developing various synthetic approaches for the fabrication of phosphorene.

Similar to other two-dimensional (2D) materials, the phosphorene preparation approaches can be divided into bottom-up and top-down methods. The schematic in Fig. 1 illustrates the two synthetic routes to monolayer and few-layer BP. The bottom-up growth strategy is based on the direct preparation of phosphorene from phosphorus precursors. There are few bottom-up approaches for the growth of thin films or few-layer BP. These methods include chemical vapor deposition (CVD) followed by high-pressure treatment, pulsed laser deposition (PLD), molecular beam epitaxy, laser writing, solution method and chemical vapor transport (CVT).[6–13] For the first time BP thin films have been obtained at room temperature by applying high-pressure on a thermally deposited red phosphorus (red-P) in a multi-anvil cell.[6] Later, BP thin films were also prepared by a similar method using a pressure vessel instead of using a multi-anvil cell.[7] The PLD method was also employed for the fabrication of ultrathin BP films on different substrates.[9] However, the BP grown using the PLD method has a highly disordered amorphous structure. Tian *et al.*[11] developed a solvothermal method for the bottom-up preparation of partially oxidized BP nanosheets. Very recently, CVT has been used for the growth of BP thin films directly on a substrate.[12,13] All the above-mentioned processes have low scalability of the final product or the quality of few-layer BP is limited due to low crystallinity. To date, these bottom-up techniques have not fulfilled the basic requirements of high-quality and scalability, which are important for its potential applications. Although researchers have a vast toolbox of well-known reagents and reaction mechanisms that can be used in the direct synthesis of thin layer graphene and transition metal dichalcogenides, this is not yet the case for the growth of high-quality and large-area phosphorene. Unlike other 2D materials, the bottom-up method for BP thin films or phosphorene growth is not completely explored due to the complex chemistry of phosphorus. The bottom-up approach needs to be further improved by optimizing the reaction conditions to obtain high-quality phosphorene. Currently, in order to obtain high-quality and scalable yields of phosphorene, the top-down method is preferably used. In the top-down method usually a chemical intercalation or mechanical force is required to break van der Waals (vdW) interactions among stacked BP layers to obtain mono or few-layers, *i.e.* phosphorene. Most of the 2D materials are prepared from their three-dimensional (3D) single crystal counterparts by using the top-down method, *e.g.*, graphene is prepared from graphite. The bulk BP single crystal is a 3D counterpart

Ziming Zhang

Ziming Zhang received his B.S. degree from Fuzhou University, China, in 2013. He completed his Ph.D. on materials chemistry in 2018 at Tsinghua University, USA, under the supervision of Assoc. Prof. Qingfeng Yan. His research interests are the synthesis and application of black phosphorus bulk crystals. He is currently a senior research scientist in the Fujian Eversun Holding Group Co., Ltd, China.

Qingfeng Yan

Qingfeng Yan received his PhD degree from the Institute of Semiconductors, Chinese Academy of Sciences, in 2003. He joined the National University of Singapore as a research fellow in August 2003. From April 2006, he worked at Nanyang Technological University and Massachusetts Institute of Technology as a joint postdoctoral fellow. Dr Yan joined the Department of Chemistry, Tsinghua University, as an associate professor in 2008. His current research interest focuses on functional crystals.

of phosphorene. In order to prepare high-quality phosphorene by using the top-down method, high-quality and large-size bulk BP single crystals are premise.

The first synthesis of bulk BP single crystals can be dated back to a century ago by using a high-pressure method.[1,14] Later, with the development of high-pressure technologies much attention was devoted to understanding the reaction mechanism. However, the high-pressure method involves sophisticated and expensive equipment, which limits the fundamental study and application exploration of BP crystals.[15–19] In addition to this growth technique, BP single crystals were also grown using other methods including recrystallization from mercury or the bismuth-flux method,[20,21] ball milling,[22–24] and the CVT reaction method.[25–35] The CVT reaction method provides a controllable way to grow large-size and high-quality bulk BP single crystals with a reasonable cost. These advantages make CVT an important method for bulk BP crystal growth. Over the past few years, researchers have achieved great advances in the CVT growth of high-quality and large-size bulk BP single crystals. Mechanism understanding is important for the controllable growth of a material. Many groups have devoted their research efforts to explore the synthesis mechanism of BP single crystals and proposed some growth models. Thorough understanding of the growth mechanism will be helpful for the controlled growth of bulk BP single crystals and create an opportunity for the direct synthesis of BP thin films or phosphorene in the near future. Recently, some articles have summarized the recent evolution in BP studies, particularly on the synthesis methods, properties and applications.[36–40] A general overview of bulk BP crystal growth by various methods has also been highlighted in some previous reviews.[41–44] However, a specific review on the CVT growth of bulk BP single crystals has not been published yet. Herein, we present a comprehensive review about the recent progress in the controllable growth of bulk BP single crystals by the CVT reaction method. The focus is on the reaction system, nucleation and growth mechanism of CVT synthesis of bulk BP single crystals. The latest advancement in the growth of doped and substituted BP bulk single crystals is also introduced. At the end of this review, we list several key challenges and opportunities in the field related to BP growth.

2. Structure and properties of BP

BP has a quite unique puckered layered structure, having features unlike most other 2D materials. The atomic planes of BP are assembled by vdW interactions. Under normal conditions, BP has an orthorhombic crystalline structure in which every phosphorus (P) atom establishes covalent interactions through sp^3 hybridization with three neighboring atoms. Two out of three covalent bonds exist in a plane while the third one connects the P atom above or below the plane. Such type of hybridization leaves a lone electron pair on each P atom, which is responsible for the quadrangular pyramid structure of P_6 rings in the chair form. The schematic illustrations in Fig. 2a–c show the lattice structure of 3D, top and side views of BP.[36] In 2014, two research groups reported the exfoliation of bulk BP crystals independently.[4,45] They applied mechanical force with the help of Scotch tape to disrupt the vdW interactions and obtain few-layer BP. Anisotropy was observed in the optical, mechanical, thermoelectric, and electrical properties of BP due to its puckered layered structure.[46–54] For example, BP exhibits a strong in-plane anisotropic response when excited with a polarized laser. Fig. 2d and e represent the angle-dependent Raman spectra of monolayer BP and A^2_g mode intensity as a function of the polarization angle.[47] BP is an ambipolar semiconductor with a thickness-dependent direct band-gap (Fig. 2f).[53] The increase in the band gap can be attributed to the charge carrier's confinement in thickness-decreased BP. Tightly bound exciton formation in 2D materials is responsible for the presence of strong Coulomb interactions.[55,56] Transition of such excitons governs the photophysics of 2D materials. Anomalous excitonic effects in BP play an important role in optical transition. BP displays many-body interaction effects and outstanding anisotropic quasiparticle properties that offer thrilling ground for new physics. These exciting properties provide excellent opportunities to fabricate practical devices for innovative applications. Most of the exfoliated vdW materials are not completely stable in air. In the case of BP the degree of degradation under ambient conditions is relatively severe. Therefore, accomplishment of its exciting potential depends on the discovery of advanced solutions to its instability.[57]

3. Synthesis of bulk BP by the CVT reaction method

The CVT reaction is an important synthetic method for the growth of pure crystalline solids. The term CVT stands for the reaction that involves the transformation of a condensed phase to a gaseous phase by a chemical reaction in the presence of a transport agent and then deposition to another place, generally in the crystalline form.[58] In 2006, Nilges's group was working on the preparation of polyphosphides by using the CVT reaction method with the addition of mineralizing agents as reaction promoters.[59] During the preparation of these polyphosphides they achieved great progress in the synthesis of BP single crystals at a relatively low temperature and pressure.[25] The discovery of this method was a great achievement in terms of material quality and synthesis simplicity. After this pioneer work, various reaction systems have been developed by different groups in order to optimize the conditions for BP crystal growth. In the below section we will thoroughly introduce the different reaction systems that have been adopted for bulk BP growth and the growth mechanism proposed by various groups.

3.1. Reaction systems for BP growth

The reaction systems for BP growth by the CVT method can be categorized into various types on the basis of the elemental

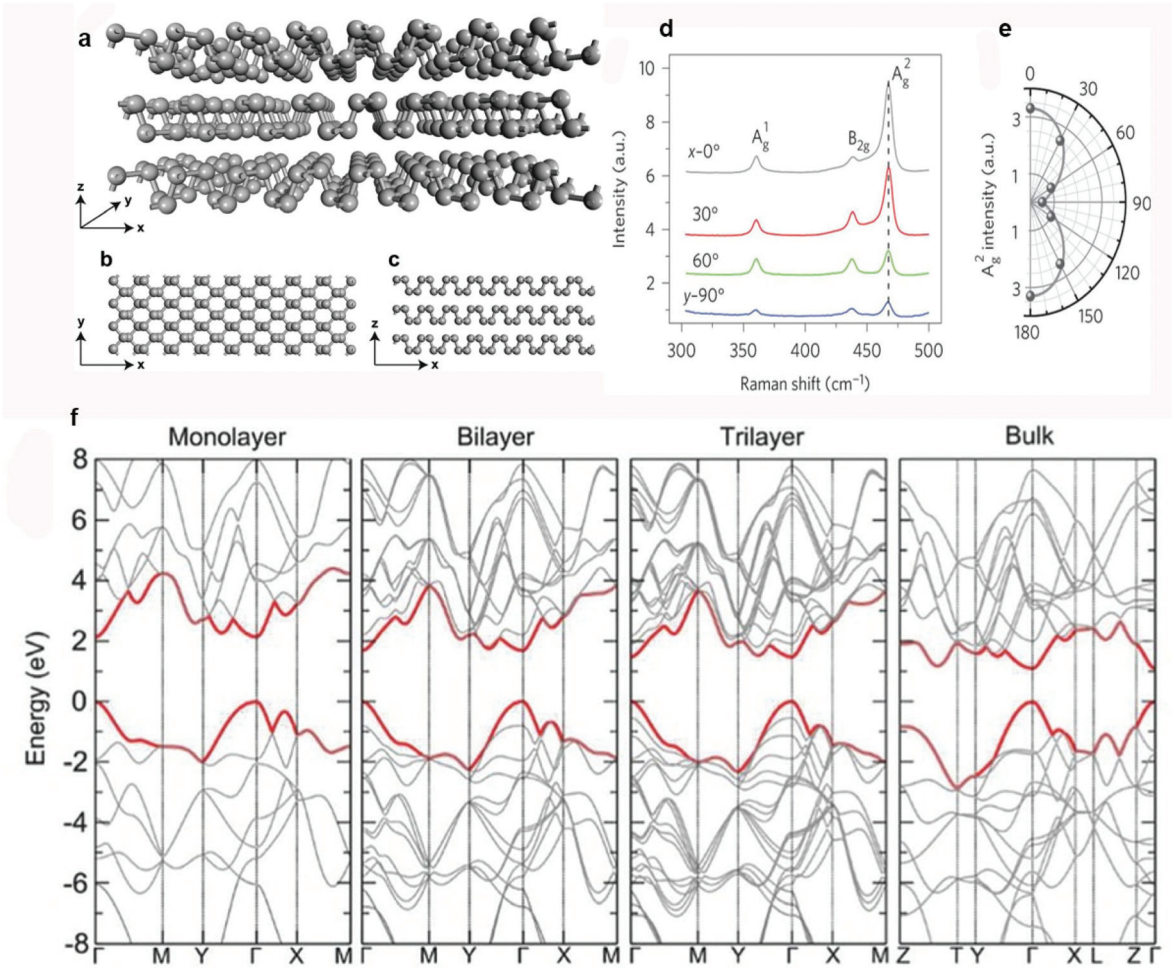

Fig. 2 Crystal structure and properties of BP. (a) Three-dimensional view. (b) View from the top. (c) View from the side. (d) Raman spectra of BP, excited by a linearly polarized laser. (e) Intensity of the A^2_g mode as a function of the polarization angle. (f) Theoretically calculated layer-dependent band structures of BP. Reproduced with permission from ref. 36, 47 and 53. Copyright 2017, The Royal society of Chemistry, 2015 Nature Publishing Group, and 2014 IOP, respectively.

composition of the mineralizers. Nilges and co-workers reported the first reaction system for bulk BP growth in the CVT reaction method.[25] In this reaction system they introduced stoichiometric amounts of gold (Au), tin (Sn), tin(IV) iodide (SnI_4) and red-P (Au/Sn/SnI_4/red-P) into an evacuated silica ampule. The silica ampule containing reactants was heated to a high temperature and kept for 5–10 days in a tube furnace. As a result, BP single crystals appeared with some additional phases such as Au_3SnP_7, AuSn, Sn_4P_3 and SnI_4. The need for long reaction time and precious metals and undesirable phases were the major problems in the Au/Sn/SnI_4/red-P system. The additional phases reduced the yield and also caused problems in the separation of pure BP crystals from the final product. Under their experimental conditions, they established that Au, Sn and I were crucial for successful synthesis. From theoretical and experimental results, they suggested that the *in situ* preparation of Au_3SnP_7, which undergoes epitactic reaction, played an important role in the conversion from red-P to BP crystals. They supposed that accelerating the *in situ* formation of Au_3SnP_7 could accelerate the reaction. Later on, they improved their previously reported reaction system by using the AuSn alloy instead of Au and Sn metals.[26] By the introduction of the AuSn/SnI_4/red-P reaction system and temperature programming the growth time was reduced from 5–10 days to 32.5 hours. Although the reaction time and unwanted byproducts were reduced to some extent, the problem of the precious metal still existed. In 2014, the same group further improved the synthesis procedure by removing the precious metal (Au) from the reaction system. The new system (Sn/SnI_4/red-P) not only reduced the synthetic cost of BP single crystals but also further reduced the unwanted phases.[27] After proper temperature programming, no significant amounts of SnI_4 and red-P were detected on BP bunches. Fig. 3a shows a photograph of a silica glass ampule containing CVT grown BP crystals. The above reaction system could produce BP crystals with sizes of several millimeters and high purity, with ability for scale-up synthesis.

However, the Sn/SnI_4/red-P system still has some limitations such as the tedious synthesis of SnI_4 and necessary temperature gradient of 45–50 °C. A fluctuation of this temp-

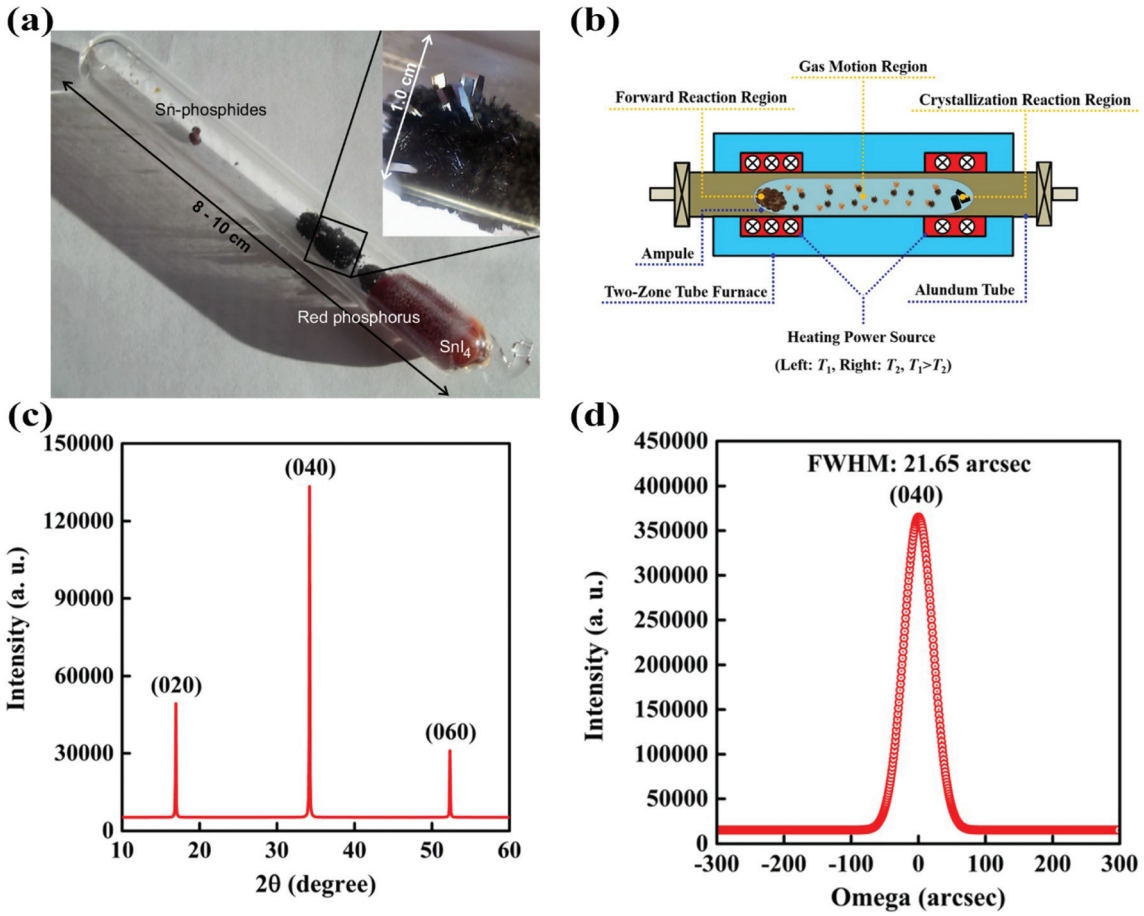

Fig. 3 (a) A silica ampule containing CVT grown BP. (b) Schematic of a tube furnace with two independent heating zones for the CVT reaction. Reproduced with the permission. (c) XRD of a BP single crystal prepared by CVT. (d) X-ray rocking curve of BP. Reprinted with permission from ref. 27 and 29. Copyright 2014 Elsevier and 2016 Springer-Verlag, respectively.

erature gradient might result in the synthesis of Hittorf's phosphorus (HP) and white phosphorus as major products. Moreover, in all previous strategies the low-pressure sealing of ampules was important for BP crystal growth. Zhao *et al.*[28] reported a facile method for the commercial production of centimeter-scale BP microribbons by introducing the Sn/I_2/red-P reaction system. They removed the condition of low-pressure sealing of ampules and replaced the tube furnace with a muffle furnace, which has a much larger reaction space. As the reaction temperature was much higher than the sublimation temperature of SnI_4, this reaction system also eliminated the tedious synthesis step of SnI_4 by replacing it with Sn and I_2.

Later in 2016, our group developed the Sn/I_2/red-P based reaction system for bulk BP crystal growth by using a two-step heating process.[29] Fig. 3b shows the schematic illustration of the tube furnace with two independent heating zones. In this method the purification process of BP crystals was greatly simplified since tin phosphide was the only byproduct, which could be removed by washing with dilute hydrochloric acid. The XRD results support the high crystallinity of BP crystals. Fig. 3c shows the XRD pattern of the CVT grown BP bulk crystal. As the quality of the BP crystal was very important for its applications, the X-ray rocking curve was employed to check the crystalline quality of the CVT grown BP crystal. As can be seen in Fig. 3d, the full width at half maximum of the BP crystal is 21.65 arc sec, demonstrating a reputable crystalline quality. The mechanically exfoliated phosphorene from the CVT grown BP crystal exhibited a record hole mobility of 1744 $cm^2\ V^{-1}\ s^{-1}$ and an excellent on/off ratio of 10^4, which was another evidence of its high crystalline quality. Although various reaction systems have been discovered but the role of specific metals and halogens remained unclear. Zhao *et al.* further developed a series of reaction systems to investigate the role of metals (or alloys) and halogens in BP crystal growth.[31] From these experiments, they observed that the specific metals (or alloys) and I_2 (or iodide containing compounds) should participate in the reaction system for the successful BP growth. However, no BP crystals were observed in the ampule by replacing iodide containing compounds with chloride compounds in the reaction system. To figure out the contribution of I_2 in BP crystal growth, they fixed the amount of red-P and specific metals. It was observed that the yield of the BP crystal was improved up to a certain level, when the

amount of I_2 was increased. These results showed that I_2 acted as a mineralizer in the CVT process, which enhanced the solubility and assisted the transfer of phosphorus. The BP yield was also affected by the nature of metals or alloys in a reaction system. It was reported that with an increase in the temperature the particular metal (or alloy) offered a liquid solution to efficiently dissolve phosphorus and precipitated it at a low temperature during the slow cooling process. If Sn was substituted by lead (Pb) in a reaction system, BP crystals also appeared in the product. The solubility of phosphorus in molten Pb considerably increased with an increase in pressure and temperature. If Sn was substituted by other metals with a low melting temperature, for example, indium (In), cadmium (Cd) or bismuth (Bi), no BP crystals were found in the products. In the case of In and Cd, the solubility of phosphorus was very low according to phase diagrams. In the case of Bi, the red-P did not dissolve in liquid Bi, which resulted in the failure of BP crystal growth. Therefore, it has been confirmed from the experimental results that the solubility of phosphorus in liquid metals (or alloys) and the presence of I element are the two key factors for the growth of BP in high yield. Very recently, Liu *et al.* have developed a short distance transport (SDT) method in the CVT-based reaction using a uniform temperature to grow high-quality BP with 98% yield.[35] In order to understand the growth mechanism of BP in this SDT process, they have performed systematic experiments with different growth parameters, including the type of transport agent, the mass ratio of Sn/SnI_4, and the growth temperature. To study whether Sn and SnI_4 are necessary reactants during the growth of BP, they also used other iodides as the reaction promoters. Wang and co-worker have claimed that the Pb/I_2/red-P reaction system gives a good quality BP as compared with the Sn/I_2/red-P reaction system.[60]

Although different reaction systems with a variety of metals (or alloys) and halogen additives have been tested, Sn and I element containing reaction systems (Sn–I assisted) are generally used for the growth of bulk BP crystals of high quality. A lot of effort has been made to unveil the mechanism of BP growth in the Sn–I assisted system. In following section, we will thoroughly explain the nucleation and growth mechanism of BP crystals synthesized by the Sn–I assisted CVT reaction.

3.2. Growth mechanism

BP crystal growth is a challenging task mainly due to inadequate mechanism understanding. Both the quality and quantity of bulk BP can be improved with better understanding of the growth mechanism. More importantly, a complete understanding of the nucleation and growth mechanism may pave the way for the direct growth of phosphorene on a substrate. Many questions might appear in mind regarding BP crystal growth by the CVT reaction method. For instance, what is the actual contribution of different mineralizers in the growth of BP crystals? Is it similar to crystallization and/or crystal growth by flux from high to low temperature? Whether it is a quite quick process that happens in a narrow temperature range? What will be the most stable species in this system under high temperature? Which kind of species provides a nucleation site to initiate the growth process? All such kinds of questions have been discussed by different groups, but many of them still need further clarification for better understanding the nucleation and growth mechanism.

Nilges's group has focused on the understanding of the growth mechanism since their first breakthrough in BP crystal growth.[25] Based on theoretical calculation results of the solid-state and gas-phase equilibrium, they excluded the thermodynamically assisted growth of BP and proposed that the BP growth preferably followed the kinetically controlled mechanism. In 2014, they further evaluated the growth of BP single crystals by *in situ* neutron diffraction experiments.[27] Fig. 4a represents the reaction time *vs.* temperature and relative peak area of the first strong reflection (040) of BP observed during the *in situ* neutron diffraction experiment. From this experiment they derived an important conclusion that the growth of BP was a fast process (complete within minutes) after initial nucleation.

After searching a variety of reaction systems by different research groups, it has been realized that Sn and I elements are critical in the CVT growth of BP crystals. Currently the Sn–I assisted reaction system is the most reliable for high-quality BP crystal growth. Regarding the Sn–I assisted system, various groups have proposed different growth mechanisms with some common opinions. For instance, Zhao *et al.* designed eleven experiments to figure out the growth mechanism of BP.[28] From these experiments they concluded that the growth of BP completed in four stages. During the first stage, when the temperature was gradually increased from 300 to 673 K, I_2 and Sn evaporated because of their low melting points. The complete ampule appeared light yellow due to the formation of tin iodide from the reaction of Sn and I_2. Unlike in a reversible reaction, the tin iodide wouldn't be decomposed into their respective elements due to the excessive Sn in the ampule. During the second stage, the sublimation of red-P began due to the increase in the temperature from 673 to 863 K and the ampule tube appeared as dark red. The Sn–P–I compound appeared in the ampule by the reaction of phosphorus gas with tin iodide and Sn. In the third step the gas inside the silica ampule began to condense because of the decrease in temperature from 863 to 798 K. In the fourth stage, the growth of BP microribbons occurred and the silica tube turned clear. Later on, they performed a series of experiments, by replacing Sn with other metals, such as In, Cd, Bi, and Pb. From the experimental observations, they proposed a molten alloy-based mechanism.[31] In this mechanism, red-P and the metal first form a molten alloy when temperature increases. Subsequently, during the constant temperature heating process, more phosphorus dissolves into the liquid eutectic Sn–P alloy. BP crystals were supposed to precipitate with a decrease in temperature from the molten Sn and red-P alloy.[28] BP crystals, synthesized by Sn–I assisted CVT reactions, typically exhibit growth sites where BP crystals cross each other (Fig. 4b).

In addition to the experimental studies, the first-principles calculations advised a BP growth mechanism based on liquid-

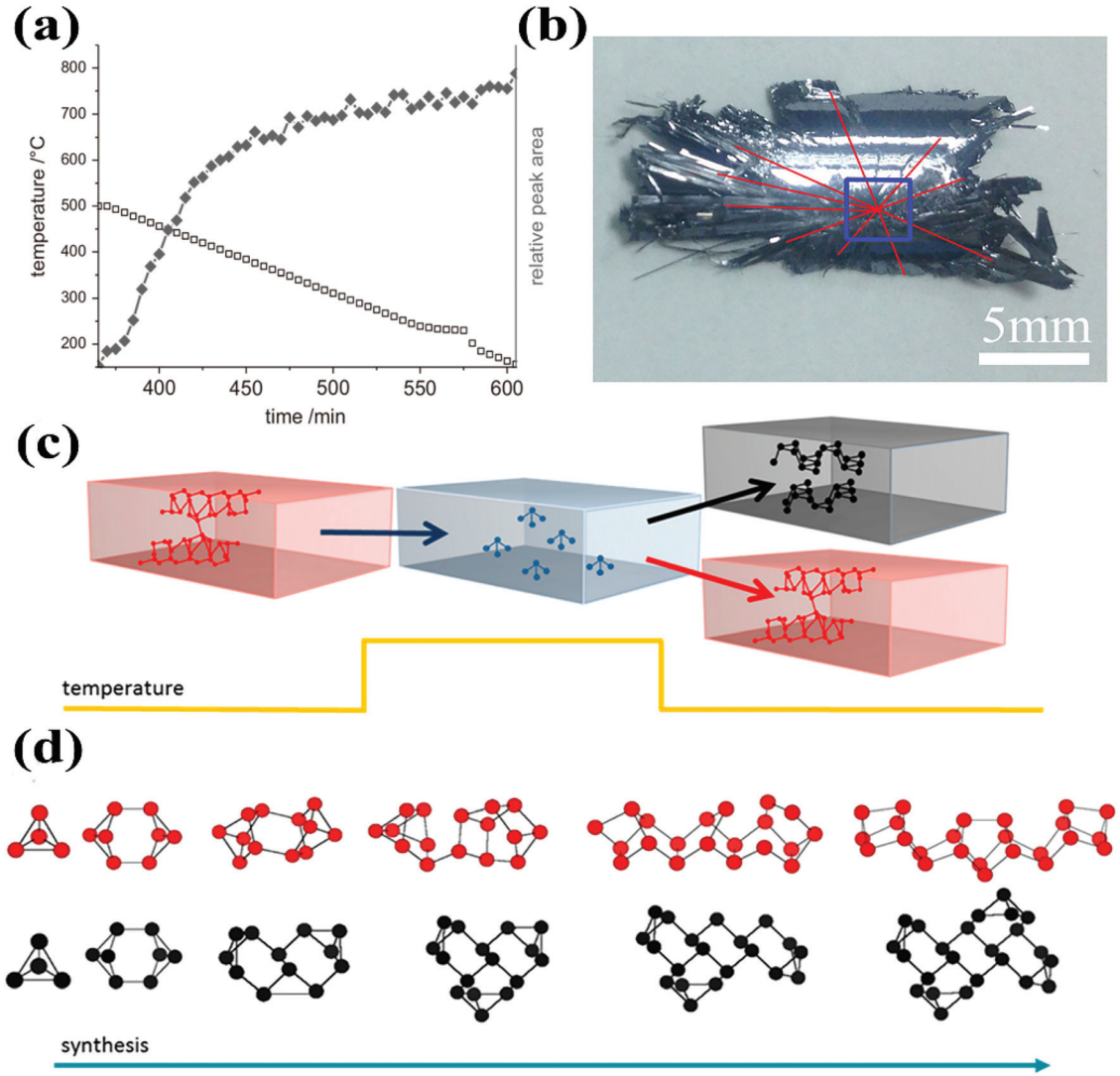

Fig. 4 (a) The reaction time *vs*. temperature and the relative peak area of first strong reflection (040) of BP observed during the *in situ* neutron diffraction experiment. (b) Photograph of the rear part of a BP crystal. The blue box indicates a growth site. (c) Schematic presentation of the proposed competing formation pathways of BP and red-P. Break-down of red-P tubes into P_4 molecules by increasing temperature and assembly of these P_4 into BP or red-P with a decrease in temperature. (d) Addition of P_4 molecules in a polymerization-like reaction to form either BP or red-P. Reprinted with permission of ref. 27, 28 and 61. Copyright 2014 Elsevier, 2016 and 2018 American Chemical Society, respectively.

to-solid transformation. To specify the reaction pathway and understanding the role of the Sn/I catalyst, Shriber *et al.* recently reported the calculated results by using dispersion-corrected density functional theory.[61] They found that the formation of red-P and BP from the P_4 molecules could be easily understood by considering the polymerization-type growth process. Fig. 4c shows the schematic of the breaking of tubular red-P into P_4 molecules followed by the reassembly of these P_4 molecules by the polymerization-like process into 2D BP sheet or back into the tubular red-P. Fig. 4d schematically illustrates the shape of the growth nuclei of BP and red-P formed by the addition of P_4 molecules in a polymerization-type reaction.[61] However, BP appeared at high-pressure or at ambient pressure in the presence of Sn and I catalysts. Both first-principles calculations[61,62] and experimental results[25–29] showed that BP was the most stable allotrope. This indicated that the failure of BP growth under ambient conditions was due to the presence of kinetic barriers. Therefore, growth of BP from red-P could be initiated by removing these barriers by using the Sn/I catalysts. After series of CVT reaction observations and product characterization, Wang *et al.* proposed the growth mechanism preferring the polymerization-type growth process.[34] In addition, they suggested that all Sn–I assisted synthesis of BP crystals shared the same reaction mechanism despite the differences among Sn and I element containing additives.

Although both the experimental and simulated results support the liquid-to-solid transformation mechanism, there are still some noteworthy deviations. One deviation is the presence of BP crystals away from the Sn–P byproducts, which specifies a transport of BP from the liquid phase to other places.[27]

In addition, the presence of the 48 atom Sn cluster assumed by the theoretical calculation has not been established experimentally.[61] Collectively, the abovementioned deviations show that the liquid–solid transformation mechanism needs to be further improved.

The most important thing in exploring the growth mechanism is to determine the detailed reaction steps involved. A better understanding of the step-by-step phase transformation is of paramount importance for the direct growth of few-layer BP. In the Sn–I assisted reaction system it is widely accepted that, with the rise in temperature, Sn, I and P first react and form a Sn–P–I compound at the cold zone. However, the stoichiometric ratio of the Sn–P–I compound was indistinct at that time.[25–28] Recently, our group proposed a phase-transfer mechanism for the Sn–I assisted CVT synthesis of BP single crystals. In this mechanism the HP was identified as an important intermediate during the transformation of red-P to BP.[30] In 2016, our group found that Sn_4P_3 and $Sn_{24}P_{19.3}I_8$ compounds appeared after heating the ampule to 460 °C.[29] In order to maintain the reaction system at high temperature, element P in the Sn–P–I compound would separate out, forming HP at the low temperature zone. In the meantime, the released I and Sn capture more P until it entirely converts into HP. Finally, the Sn–P–I compound adsorb on the surface of HP, acting as catalytic sites to convert HP to BP. These findings were precisely established with a series of optical and structural characterization and also reinforced by quantum chemical calculations.[30] Fig. 5a demonstrates the schematic of the phase-transfer mechanism. Micro-Raman spectroscopy was utilized to study the composition of the crystal which was obtained by a modified CVT reaction. Fig. 5b represents the Raman spectra of the sample around the phase boundary. The phase boundary between BP and HP can be distinguished. The vibrations of BP phonon modes appear on the phase boundary, as illustrated in Fig. 5c–e. In our study the actual time of the phase transition was absent. Later, a series of interference experiments was designed to determine the time of the phase transitions between red-P, HP and BP during the CVT reaction.[32] However, this mechanism is primarily based on the characterization of the as-grown products prepared by modified CVT reactions with low purity. The supporting evidence would be more convincing if *in situ* characterization can be conducted. The phase-transfer mechanism, in which HP is supposed to be the critical intermediate state, still needs further refinement.

Later in 2017, Li *et al.* suggested a vapor–solid–solid mechanism, in which BP formed with the assistance of the Sn–P–I compound.[33] Two phases of Sn, P, and I based ternary compounds have been reported to date. One of them is SnIP with a double helix structure while the other is the ternary inverse clathrate with $Sn_{24}P_{19.3}I_8$ composition.[63–66] According to this mechanism the intrinsic P vacancies in the crystal structure of $Sn_{24}P_{19.3}I_8$ played an important role in BP growth. They proposed that when the temperature was lower than 520 °C, only Sn–P–I was stable under these conditions. The temperature gradient provides the driving force for the movement of this clathrate from the source region to the product region in an ampule. This inverse type-I clathrate acted as a nucleation site for the growth of BP in the product region of an ampule. After formation of this stable compound the P_4 started its decomposition at the surface of this compound and P atoms diffused in the structure. When the amount of absorbed P was high enough in $Sn_{24}P_{19.3}I_8$, P started its segregation at some location on the surface of $Sn_{24}P_{19.3}I_8$ as BP. As time went on, the BP crystal grew gradually. Chen *et al.* compared the crystal structure of BP and $Sn_{24}P_{19.3}I_8$.[32] The structure of BP along the (020), (040) and (060) planes has ring-like fragments, which are similar to those observed in $Sn_{24}P_{19.3}I_8$ along the (600) plane (Fig. 6a). Thus, the epitaxial growth of BP on $Sn_{24}P_{19.3}I_8$

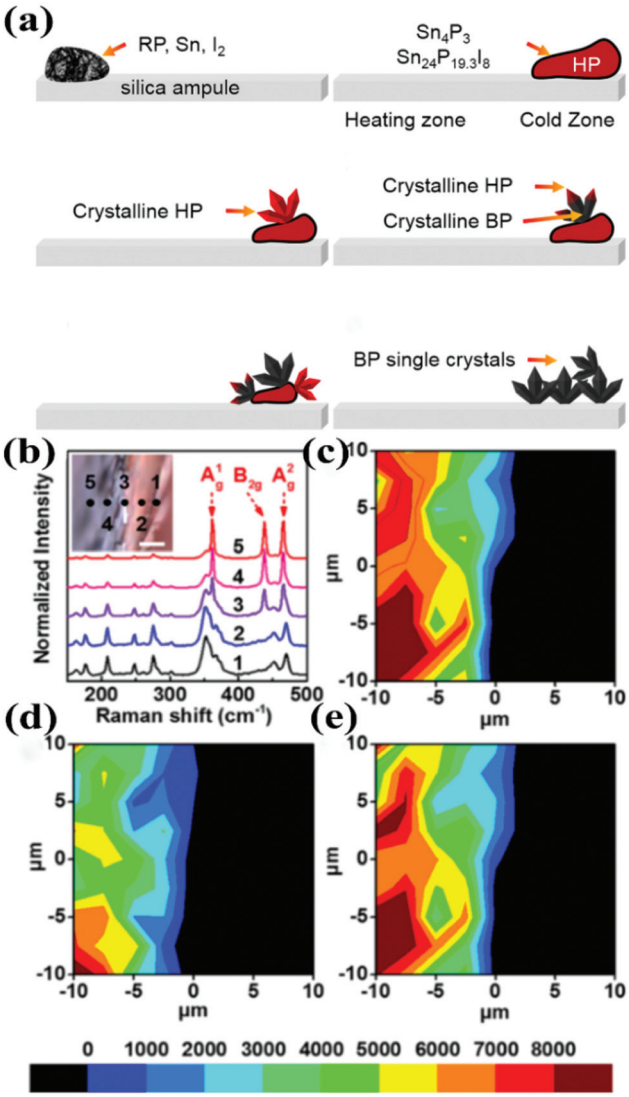

Fig. 5 (a) Schematic diagram of phase transition from red-P to BP. (b) Raman spectra of the sample around the phase boundary. The inset is an OM image of the phase boundary; the scale bar is 5 μm. (c) A^1_g phonon mode. (d) B^2_g phonon mode. (e) A^2_g phonon mode Raman intensity mapping images, corresponding to the OM image of the inset of (b). Reproduced with permission from ref. 30. Copyright 2017 The Royal Society of Chemistry.

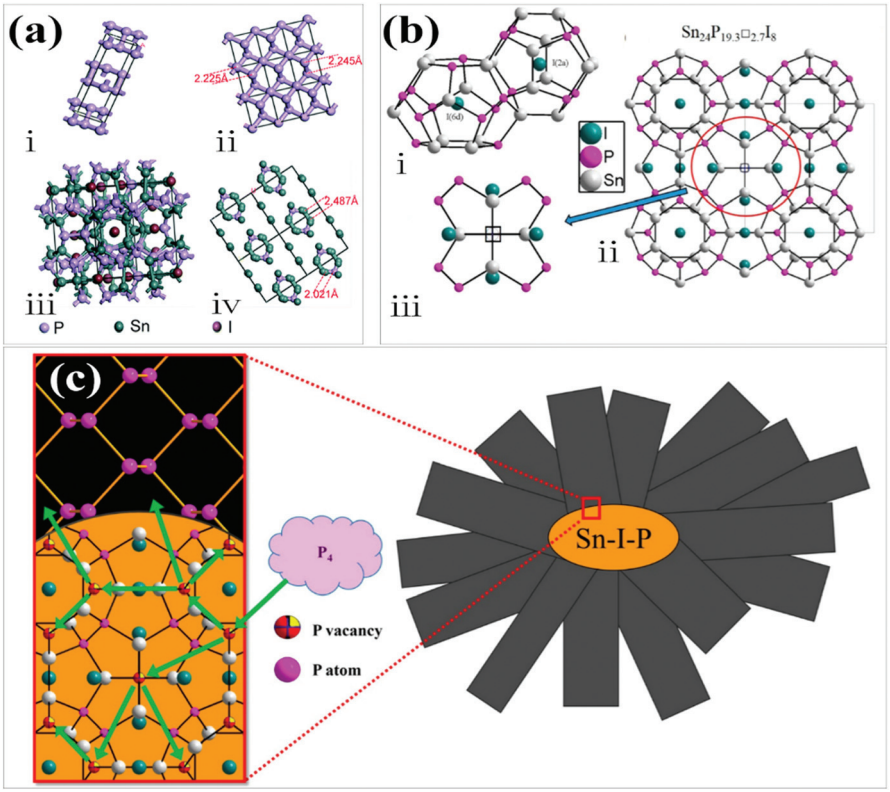

Fig. 6 (a) (i) BP unit cell, (ii) ring-like fragments of BP (viewed along the (020), (040) and (060) planes), (iii) the unit cell of $Sn_{24}P_{19.3}I_8$ and (iv) ring-like fragments of $Sn_{24}P_{19.3}I_8$ (viewed along the (600) plane). (b) (i) Pentagonal dodecahedra and tetrakaidecahedron frameworks formed by Sn and P atoms in the clathrate $Sn_{24}P_{22-x}I_8$ and (ii, iii) the crystal structure of $Sn_{24}P_{22-x}I_8$. (c) Schematic of the proposed growth mechanism. Reproduced with the permission from ref. 32 and 33. Copyright 2017 The Royal Society of Chemistry and 2017 American Chemical Society, respectively.

is possible. The intrinsic P vacancies in the $Sn_{24}P_{19.3}I_8$ crystal structure play an important role in BP growth. It was reported that the vacancies at the P sites in the framework of $Sn_{24}P_{19.3}I_8$ might hold the glue for its catalytic effect to grow BP crystals through the direct interaction of P vapor with this solid clathrate in the ampule (Fig. 6b and c).[33]

The above BP crystal growth mechanisms in CVT reactions were proposed mainly based on experimental observations under different reaction conditions. Although they share some common opinions, these suggested that mechanisms are different from each other with distinct reaction pathways. Additional efforts are therefore still needed to reveal the conversion from red phosphorus to BP in the CVT reaction systems.

4. Doping and substitution in BP

Doping and substitution are two common strategies that have been used for manipulating the properties of materials. Generally, doping involves the replacement in a crystal lattice by another element from different groups in the periodic table. In contrast to doping, substitution means that the element is partially substituted by another element (from the same group of the periodic table) and forms a stable configuration. To tune the properties of BP the incorporation of the foreign element has been demonstrated by different groups using various methods.[67–73] It was observed that arsenic (As) could be incorporated into BP by using the CVT reaction with tunable compositions.[67] Moreover, the As-substitution in BP retained the semiconductor characteristics of the BP crystal. Antimony (Sb) substitution in the BP crystal was also tried using the CVT reaction method by Nilges's group, but they were not successful in the substitution of Sb into the BP crystal structure due to the large difference in the atom radius of two elements. Interestingly, they succeeded in the growth of Sb-substituted HP during this experiment.[71]

The CVT reaction method has also been employed for the doping of selenium (Se) in BP crystals. Xu *et al.* reported that Se-doping showed an enhancement of photoelectrical properties of BP.[68] Liu's group successfully doped 0.1% tellurium (Te) in BP by using the high-pressure method. Te-doping improved the performance, especially the ambient stability of BP-based field-effect transistors.[70] Recently, our group reported the Te-doping in BP bulk crystals with the CVT reaction method, which allowed uniform doping with a quite large amount (0.5% atomic ratio).[73] Very recently, Liu and co-workers have developed a powerful SDT method in the CVT reaction using a uniform temperature to grow doped BP with

the highest growth yield.[35] They have revealed experimentally and theoretically that doping with a suitable element could be an effective strategy to improve the chemical stability of BP.

5. Conclusion and perspectives

Due to its promising physical and chemical properties, phosphorene has tremendous applications in the field of electronics, optoelectronics and biomedicine. Research interest in phosphorene has stimulated the rapid development in the growth of bulk BP single crystals, which serve as a reliable precursor for the top-down preparation of phosphorene. The past few years have witnessed a number of encouraging advancements in the quality and yield improvement of bulk BP single crystals by searching new reaction systems and proper understanding of the nucleation and growth mechanism in the CVT reaction method. This brief review highlights the recent advances in the growth of bulk BP crystals by using the CVT reaction method.

In order to integrate phosphorene into practical devices, its scalable fabrication is critical. So far, CVD is the primary method for the large area growth of 2D materials. In a previous study few groups have employed some techniques for the growth of BP thin films. Among these techniques, CVT-grown BP thin films show larger lateral size and better crystalline quality. However, still these techniques have not fulfilled all the commercialization requirements. Therefore, it is essential to develop a rational method for the growth of high-quality phosphorene. By thoroughly understanding the nucleation and growth process, the CVT method is expected to be a promising technique towards few-layer BP synthesis.[13] The CVD is another chemical vapor-based method and has been extensively used for large-area 2D material synthesis. In a typical CVD method, chemical vapors react on a specific substrate surface to produce the required materials, which is quite similar to CVT. A carrier gas is introduced in the CVD method, which makes the system more complicated, as compared with CVT. Despite these differences, both reactions can yield the products by deposition from the gaseous phase. Therefore, the understanding and expertise obtained in CVT can help to develop a CVD-based method for 2D BP preparation.

Furthermore, one of the major problems with phosphorene is its sensitivity to an ambient atmosphere. Few-layer BP degrades very quickly under ambient conditions due to the moisture and oxygen in air. Therefore, it is very important to enhance the stability by applying some strategies. One of such strategies is doping in BP. Previous studies have shown that doping in BP bulk single crystals by using CVT not only changes the electrical properties of BP but also improves the moisture stability.[70] Optimizing the doping process or trying other elements by using the CVT reaction method may be helpful in improving the stability of exfoliated phosphorene. Considering many advantages of the CVT reaction method, we have great expectations for the future development of growth of BP single crystals and their derivatives.

Conflicts of interest

The authors declare no conflict of interest.

Acknowledgements

This work was supported by the National Natural Science Foundation of China (No. 21671115), the Science Challenge Project (TZ2018004), the Innovation Center of Radiation Application (KFZC2018040204), and the Tsinghua University Initiative Scientific Research Program (2018Z05JZY022).

References

1 P. W. Bridgman, Two new modifications of phosphorus, *J. Am. Chem. Soc.*, 1914, **36**, 1344–1363.
2 M. Engel, M. Steiner and P. Avouris, Black phosphorus photodetector for multispectral, high-resolution imaging, *Nano Lett.*, 2014, **14**, 6414–6417.
3 W. Zhu, M. N. Yogeesh, S. Yang, S. H. Aldave, J.-S. Kim, S. Sonde, L. Tao, N. Lu and D. Akinwande, Flexible black phosphorus ambipolar transistors, circuits and AM demodulator, *Nano Lett.*, 2015, **15**, 1883–1890.
4 L. Li, Y. Yu, G. J. Ye, Q. Ge, X. Ou, H. Wu, D. Feng, X. H. Chen and Y. Zhang, Black phosphorus field-effect transistors, *Nat. Nanotechnol.*, 2014, **9**, 372–377.
5 M. Zhu, S. Kim, L. Mao, M. Fujitsuka, J. Zhang, X. Wang and T. Majima, Metal-free photocatalyst for H_2 evolution in visible to near-infrared region: black phosphorus/graphitic carbon nitride, *J. Am. Chem. Soc.*, 2017, **139**, 13234–13242.
6 X. Li, B. Deng, X. Wang, S. Chen, M. Vaisman, S.-I. Karato, G. Pan, M. L. Lee, J. Cha and H. Wang, Synthesis of thin-film black phosphorus on a flexible substrate, *2D Mater.*, 2015, **2**, 031002.
7 J. B. Smith, D. Hagaman and H.-F. Ji, Growth of 2D black phosphorus film from chemical vapor deposition, *Nanotechnology*, 2016, **27**, 215602.
8 C. Li, Y. Wu, B. Deng, Y. Xie, Q. Guo, S. Yuan, X. Chen, M. Bhuiyan, Z. Wu, K. Watanabe, T. Taniguchi, H. Wang, J. J. Cha, M. Snure, Y. Fei and F. Xia, Synthesis of crystalline black phosphorus thin film on sapphire, *Adv. Mater.*, 2018, **30**, 1703748.
9 Z. Yang, J. Hao, S. Yuan, S. Lin, H. M. Yau, J. Dai and S. P. Lau, Field-effect transistors based on amorphous black phosphorus ultrathin films by pulsed laser deposition, *Adv. Mater.*, 2015, **27**, 3748–3754.
10 G. Qiu, Q. Nian, M. Motlag, S. Jin, B. Deng, Y. Deng, A. R. Charnas, P. D. Ye and G. J. Cheng, Ultrafast laser-shock-induced confined metaphase transformation for direct writing of black phosphorus thin films, *Adv. Mater.*, 2018, **30**, 1704405.
11 B. Tian, B. Tian, B. Smith, M. C. Scott, Q. Lei, R. Hua, Y. Tian and Y. Liu, Facile bottom-up synthesis of partially oxidized black phosphorus nanosheets as metal-free photo-

catalyst for hydrogen evolution, *Proc. Natl. Acad. Sci. U. S. A.*, 2018, **115**, 4345–4350.
12 N. Izquierdo, J. C. Myers, N. C. A. Seaton, S. K. Pandey and S. A. Campbell, Thin film deposition of surface passivated black phosphorus, *ACS Nano*, 2019, **13**, 7091–7099.
13 Y. Xu, X. Shi, Y. Zhang, H. Zhang, Q. Zhang, Z. Huang, X. Xu, J. Guo, H. Zhang, L. Sun, Z. Zeng, A. Pan and K. Zhang, Epitaxial nucleation and lateral growth of high-crystalline black phosphorusfilms on silicon, *Nat. Commun.*, 2020, **11**, 1330.
14 P. W. Bridgman, Further note on black phosphorus, *J. Am. Chem. Soc.*, 1916, **38**, 609–612.
15 R. Hultgren, N. S. Gingrich and B. E. Warren, The atomic distribution in red and black phosphorus and the crystal structure of black phosphorus, *J. Chem. Phys.*, 1935, **3**, 351–355.
16 A. Brown and S. Rundqvist, Refinement of the crystal structure of black phosphorus, *Acta Crystallogr.*, 1965, **19**, 684–685.
17 I. Shirotani, Growth of large single crystals of black phosphorus at high pressures and temperatures, and its electrical properties, *Mol. Cryst. Liq. Cryst.*, 1982, **86**, 203–211.
18 L.-Q. Sun, M.-J. Li, K. Sun, S.-H. Yu, R.-S. Wang and H.-M. Xie, Electrochemical activity of black phosphorus as an anode material for lithium-ion batteries, *J. Phys. Chem. C*, 2012, **116**, 14772–14779.
19 Q. Sun, X. Zhao, Y. Feng, Y. Wu, Z. Zhang, X. Zhang, X. Wang, S. Feng and X. Liu, Pressure quenching: a new route for the synthesis of black phosphorus, *Inorg. Chem. Front.*, 2018, **5**, 669–674.
20 M. Baba, F. Izumida, Y. Takeda and A. Morita, Preparation of black phosphorus single crystals by a completely closed bismuth-flux method and their crystal morphology, *Jpn. J. Appl. Phys.*, 1989, **28**, 1019–1022.
21 Y. Maruyama, S. Suzuki, T. Osaki, H. Yamaguchi, S. Sakai, K. Nagasato and I. Shirotani, Electronic properties of black phosphorus single crystals and intercalation compounds, *Bull. Chem. Soc. Jpn.*, 1986, **59**, 1067–1071.
22 M. Nagao, A. Hayashi and M. Tatsumisago, All-solid-state lithium secondary batteries with high capacity using black phosphorus negative electrode, *J. Power Sources*, 2011, **196**, 6902–6905.
23 C.-M. Park and H.-J. Sohn, Black phosphorus and its composite for lithium rechargeable batteries, *Adv. Mater.*, 2007, **19**, 2465–2468.
24 J. Sun, G. Zheng, H.-W. Lee, N. Liu, H. Wang, H. Yao, W. Yang and Y. Cui, Formation of stable phosphorus-carbon bond for enhanced performance in black phosphorus nanoparticle-graphite composite battery anodes, *Nano Lett.*, 2012, **14**, 4573–4580.
25 S. Lange, P. Schmidt and T. Nilges, Au_3SnP_7@black phosphorus: an easy access to black phosphorus, *Inorg. Chem.*, 2007, **46**, 4028–4035.
26 T. Nilges, M. Kersting and T. Pfeifer, A fast low-pressure transport route to large black phosphorus single crystals, *J. Solid State Chem.*, 2008, **181**, 1707–1711.
27 M. Köpf, N. Eckstein, D. Pfister, C. Grotz, I. Krüger, M. Greiwe, T. Hansen, H. Kohlmann and T. Nilges, Access and in situ growth of phosphorene-precursor black phosphorus, *J. Cryst. Growth*, 2014, **405**, 6–10.
28 M. Zhao, H. Qian, X. Niu, W. Wang, L. Guan, J. Sha and Y. Wang, Growth mechanism and enhanced yield of black phosphorus microribbons, *Cryst. Growth Des.*, 2016, **16**, 1096–1103.
29 Z. Zhang, X. Xin, Q. Yan, Q. Li, Y. Yang and T.-L. Ren, Two-step heating synthesis of sub-3 millimeter-sized orthorhombic black phosphorus single crystal by chemical vapor transport reaction method, *Sci. China Mater.*, 2016, **59**, 122–134.
30 Z. Zhang, D.-H. Xing, J. Li and Q. Yan, Hittorf's phosphorus: the missing link during transformation of red phosphorus to black phosphorus, *CrystEngComm*, 2017, **19**, 905–909.
31 M. Zhao, X. Niu, L. Guan, H. Qian, W. Wang, J. Sha and Y. Wang, Understanding the growth of black phosphorus Crystals, *CrystEngComm*, 2016, **18**, 7737–7744.
32 Z. Chen, Y. Zhu, J. Lei, W. Liu, Y. Xu and P. Feng, A stage-by-stage phase-induction and nucleation of black phosphorus from red phosphorus under low-pressure mineralization, *CrystEngComm*, 2017, **19**, 7207–7212.
33 S. Li, X. Liu, X. Fan, Y. Ni, J. Miracle, N. Theodoropoulou, J. Sun, S. Chen, B. Lv and Q. Yu, New strategy for black phosphorus crystal growth through ternary clathrate, *Cryst. Growth Des.*, 2017, **17**, 6579–6585.
34 D. Wang, P. Yi, L. Wang, L. Zhang, H. Li, M. Lu, X. Xie, L. Huang and W. Huang, Revisiting the growth of black phosphorus in Sn-I assisted reactions, *Front. Chem.*, 2019, **7**, 21.
35 M. Liu, S. Feng, Y. Hou, S. Zhao, L. Tang, J. Liu, F. Wang and B. Liu, High yield growth and doping of black phosphorus with tunable electronic properties, *Mater. Today*, 2020, **36**, 91–101.
36 W. Lei, G. Liu, J. Zhang and M. Liu, Black phosphorus nanostructures: recent advances in hybridization, doping and functionalization, *Chem. Soc. Rev.*, 2017, **46**, 3492–3509.
37 Y. Zhang, Y. Zheng, K. Rui, H. H. Hng, K. Hippalgaonkar, J. Xu, W. Sun, J. Zhu, Q. Yan and W. Huang, 2D black phosphorus for energy storage and thermoelectric applications, *Small*, 2017, **13**, 1700661.
38 Y. Yi, Z. Sun, J. Li, P. K. Chu and X.-F. Yu, Optical and optoelectronic properties of black phosphorus and recent photonic and optoelectronic applications, *Small Methods*, 2019, **3**, 1900165.
39 B. Li, C. Lai, G. Zeng, D. Huang, L. Qin, M. Zhang, M. Cheng, X. Liu, H. Yi, C. Zhou, F. Huang, S. Liu and Y. Fu, Black phosphorus, a rising star 2D nanomaterial in the post graphene era: synthesis, properties, modifications, and photocatalysis applications, *Small*, 2019, **15**, 1804565.
40 M. Batmunkh, M. Bat-Erdene and J. G. Shapter, Phosphorene and phosphorene-based materials-prospects for future applications, *Adv. Mater.*, 2016, **28**, 8586–8617.

41 V. Eswaraiah, Q. Zeng, Y. Long and Z. Liu, Black phosphorus nanosheets: synthesis, characterization and applications, *Small*, 2016, **12**, 3480–3502.
42 R. Gusmão, Z. Sofer and M. Pumera, Black phosphorus rediscovered: from bulk material to monolayers, *Angew. Chem., Int. Ed.*, 2017, **56**, 8052–8072.
43 D. Wang, F. Luo, M. Lu, X. Xie, L. Huang and W. Huang, Chemical vapor transport reactions for synthesizing layered materials and their 2D counterparts, *Small*, 2019, **15**, 1804404.
44 T. Nilges, P. Schmidt and R. Weihrich, Phosphorus: the allotropes, stability, synthesis, and selected applications, *Encycl. Inorg. Bioinorg. Chem.*, 2018, DOI: 10.1002/9781119951438.eibc2643.
45 H. Liu, A. T. Neal, Z. Zhu, Z. Luo, X. Xu, D. Tománek and P. D. Ye, Phosphorene: an unexplored 2D semiconductor with a high hole mobility, *ACS Nano*, 2014, **8**, 4033–4041.
46 F. Xia, H. Wang and Y. Jia, Rediscovering black phosphorus as an anisotropic layered material for optoelectronics and electronics, *Nat. Commun.*, 2014, **5**, 4458.
47 X. Wang, A. M. Jones, K. L. Seyler, V. Tran, Y. Jia, H. Zhao, H. Wang, L. Yang, X. Xu and F. Xia, Highly anisotropic and robust excitons in monolayer black phosphorus, *Nat. Nanotechnol.*, 2015, **10**, 517–521.
48 T. Low, A. S. Rodin, A. Carvalho, Y. Jiang, H. Wang, F. Xia and A. H. C. Neto, Tunable optical properties of multilayer black phosphorus thin films, *Phys. Rev. B: Condens. Matter Mater. Phys.*, 2014, **90**, 075434.
49 J. Qiao, X. Kong, Z.-X. Hu, F. Yang and W. Ji, High-mobility transport anisotropy and linear dichroism in few-layer black phosphorus, *Nat. Commun.*, 2014, **5**, 4475.
50 H. Kim, Effect of van der Waals interaction on the Structural and cohesive properties of black phosphorus, *J. Korean Phys. Soc.*, 2014, **64**, 547–553.
51 G. Qin, Q.-B. Yan, Z. Qin, S.-Y. Yue, H.-J. Cui, Q.-R. Zheng and G. Su, Hinge-like structure induced unusual properties of black phosphorus and new strategies to improve the thermoelectric performance, *Sci. Rep.*, 2014, **4**, 6946.
52 J. Zhang, H. J. Liu, L. Cheng, J. Wei, J. H. Liang, D. D. Fan, J. Shi, X. F. Tang and Q. J. Zhang, Phosphorene nanoribbon as a promising candidate for thermoelectric applications, *Sci. Rep.*, 2014, **4**, 6452.
53 A. Castellanos-Gomez, L. Vicarelli, E. Prada, J. O. Island, K. L. Narasimha-Acharya, S. I. Blanter, D. J. Groenendijk, M. Buscema, G. A. Steele, J. V. Alvarez, H. W. Zandbergen, J. J. Palacios and H. S. J. van der Zant, Isolation and characterization of few-layer black phosphorus, *2D Mater.*, 2014, **1**, 025001.
54 H. Yuan, X. Liu, F. Afshinmanesh, W. Li, G. Xu, J. Sun, B. Lian, A. G. Curto, G. Ye, Y. Hikita, Z. Shen, S.-C. Zhang, X. Chen, M. Brongersma, H. Y. Hwang and Y. Cui, Polarization-sensitive broadband photodetector using a black phosphorus vertical p–n junction, *Nat. Nanotechnol.*, 2015, **10**, 707–713.
55 Z. Ye, T. Cao, K. O'Brien, H. Zhu, X. Yin, Y. Wang, S. G. Louie and X. Zhang, Probing excitonic dark states in single-layer tungsten disulphide, *Nature*, 2014, **513**, 214–218.
56 J. A. Schuller, S. Karaveli, T. Schiros, K. He, S. Yang, L. Kymissis, J. Shan and R. Zia, Orientation of luminescent excitons in layered nanomaterials, *Nat. Nanotechnol.*, 2013, **8**, 271–276.
57 J. Pei, X. Gai, J. Yang, X. Wang, Z. Yu, D. Y. Choi, B. Lutherdavies and Y. Lu, Producing air-stable monolayers of phosphorene and their defect engineering, *Nat. Commun.*, 2016, **7**, 10450.
58 M. Binnewies, M. Schmidt and P. Schmidt, Chemical vapor transport reactions-arguments for choosing a suitable transport agent, *Z. Anorg. Allg. Chem.*, 2017, **643**, 1295–1311.
59 S. Lange, C. P. Sebastian, L. Zhang, H. Eckert and T. Nilges, Ag_3SnCuP_{10}: $[Ag_3Sn]$ tetrahedra embedded between adamantane-type $[P_{10}]$ cages, *Inorg. Chem.*, 2006, **45**, 5878–5885.
60 Y. Yu, B. Xing, D. Wang, L. Guan, X. Niu, J. Yao, X. Yan, S. Zhang, Y. Liu, X. Wu, J. Sha and Y. Wang, Improvement in the quality of black phosphorus by selecting a mineralizer, *Nanoscale*, 2019, **11**, 20081–20089.
61 P. Shriber, A. Samanta, G. D. Nessim and I. Grinberg, First-principles investigation of black phosphorus synthesis, *J. Phys. Chem. Lett.*, 2018, **9**, 1759–1764.
62 F. Bachhuber, J. von Appen, R. Dronskowski, P. Schmidt, T. Nilges, A. Pfitzner and R. Weihrich, The extended stability range of phosphorus allotropes, *Angew. Chem., Int. Ed.*, 2015, **53**, 11629–11633.
63 D. Pfister, K. Schäfer, C. Ott, B. Gerke, R. Pöttgen, O. Janka, M. Baumgartner, A. Efimova, A. Hohmann, P. Schmidt, S. Venkatachalam, L. van Wüllen, U. Schürmann, L. Kienle, V. Duppel, E. Parzinger, B. Miller, J. Becker, A. Holleitner, R. Weihrich and T. Nilges, Inorganic double helices in semiconducting SnIP, *Adv. Mater.*, 2016, **28**, 9783–9791.
64 M. M. Shatruk, K. A. Kovnir, A. V. Shevelkov, I. A. Presniakov and B. A. Popovkin, First tin pnictide halides $Sn_{24}P_{19.3}I_8$ and $Sn_{24}As_{19.3}I_8$: synthesis and the clathrate-I type of the crystal structure, *Inorg. Chem.*, 1999, **38**, 3455–3457.
65 V. V. Novikov, A. V. Matovnikov, D. V. Avdashchenko, N. V. Mitroshenkov, E. Dikarev, S. Takamizawa, M. A. Kirsanova and A. V. Shevelkov, Low-temperature structure and lattice dynamics of the thermoelectric clathrate $Sn_{24}P_{19.3}I_8$, *J. Alloys Compd.*, 2012, **520**, 174–179.
66 M. A. Kirsanova and A. V. Shevelkov, Clathrates and semiclathrates of type-I: crystal structure and superstructures, *Z. Kristallogr. - Cryst. Mater.*, 2013, **228**, 215–227.
67 O. Osters, T. Nilges, F. Bachhuber, F. Pielnhofer, R. Weihrich, M. Schöneich and P. Schmidt, Synthesis and identification of metastable compounds: black arsenic—science or fiction?, *Angew. Chem., Int. Ed.*, 2012, **51**, 2994–2997.
68 Y. Xu, J. Yuan, L. Fei, X. Wang, Q. Bao, Y. Wang, K. Zhang and Y. Zhang, Selenium-doped black phosphorus for high-

responsivity 2D photodetectors, *Small*, 2016, **12**, 5000–5007.

69 Y. Ge, C. Si, Y. Xu, Z. He, Z. Liang, Y. Chen, Y. Song, D. Fan, K. Zhang and H. Zhang, Few-layer selenium-doped black phosphorus: synthesis, nonlinear optical properties and ultrafast photonics applications, *J. Mater. Chem. C*, 2017, **25**, 6129–6135.

70 B. Yang, B. Wan, Q. Zhou, Y. Wang, W. Hu, W. Lv, Q. Chen, Z. Zeng, F. Wen, J. Xiang, S. Yuan, J. Wang, B. Zhang, W. Wang, J. Zhang, B. Xu, Z. Zhao, Y. Tian and Z. Liu, Te-doped black phosphorus field-effect transistors, *Adv. Mater.*, 2016, **28**, 9408–9415.

71 F. Baumer, Y. Ma, C. Shen, A. Zhang, L. Chen, Y. Liu, D. Pfister, T. Nilges and C. Zhou, Synthesis, characterization, and device application of antimony-substituted violet phosphorus: a layered material, *ACS Nano*, 2017, **11**, 4105–4113.

72 B. Liu, M. Köpf, A. N. Abbas, X. Wang, Q. Guo, Y. Jia, F. Xia, R. Weihrich, F. Bachhuber, F. Pielnhofer, H. Wang, R. Dhall, S. B. Cronin, M. Ge, X. Fang, T. Nilges and C. Zhou, Black arsenic–phosphorus: layered anisotropic infrared semiconductors with highly tunable compositions and properties, *Adv. Mater.*, 2015, **27**, 4423–4429.

73 Z. Zhang, M. Khurram, Z. Sun and Q. Yan, Uniform tellurium doping in black phosphorus single crystals by chemical vapor transport, *Inorg. Chem.*, 2018, **57**, 4098–4103.